ISIJ International, Vol. 30 (1990), No. 8, pp. 674-679

Effects of Alloying Additions on Fe–Mn–Si Shape Memory Alloys

Hiroaki OTSUKA, Hiroyuki YAMADA, Tadakatsu MARUYAMA, Hiroyuki TANAHASHI, Shoichi MATSUDA[1] and Masato MURAKAMI[2]

R & D Laboratories-I, Nippon Steel Corporation, Ida, Nakahara-ku, Kawasaki, Kanagawa-ken, 211 Japan. 1) Nippon Steel Corporation. Now at Nagoya Institute of Technology, Gokiso-cho, Showa-ku, Nagoya, Aichi-ken, 464 Japan. 2) Nippon Steel Corporation. Now at Super-conductivity Research Laboratory, Shinonome, Koto-ku, Tokyo, 135 Japan.

(Received on December 1, 1989; accepted in the final form on March 9, 1990)

Fe–Mn–Si alloys are shape memory alloys which make use of the $\gamma \rightarrow \varepsilon$ stress-induced martensitic transformation. In this study, we report the effects of alloying additions on the shape memory effect (SME) of these alloys. It was found that the *Ms* temperature, the Néel temperature (T_N) and the volume of stress-induced martensite govern the SME. Through the optimization of these factors we found that new alloy systems such as Fe–28Mn–6Si–5Cr, Fe–20Mn–5Si–8Cr–5Ni and Fe–16Mn–5Si–12Cr–5Ni alloys could exhibit good SME along with good corrosion resistance. And it was also found that the thermomechanical treatment which improved the SME in Fe–Mn–Si base system was also effective to improve the SME of these new systems.

KEY WORDS: Fe–Mn–Si alloy; shape memory ferrous alloy; shape memory effect; stress-induced $\gamma \rightarrow \varepsilon$ martensitic transformation; *Ms* temperature; Néel temperature (T_N); the amount of ε phase; training effect.

1. Introduction

The phenomenon of shape recovery was discovered in Au–Cd alloy by Chang and Read in 1951.[1] Since then it had been found that Ti–Ni, Cu–Zn–Al and several other alloy systems showed shape memory effect and the effect was associated with a thermoelastic martensitic transformation. Because of high potential applications research and development of the shape memory alloys have been made worldwide.[2-4]

It is also known that several ferrous alloys also exhibit SME such as Fe–Pd[5], Fe–Pt (fcc–fct)[6], Fe–Ni–C[7], Fe–Ni–Ti–Co (fcc–bct)[8] and Fe–Ni–Cr[9], although shape recovery has been incomplete. Recently, Sato *et al.*[10-12] have discovered that complete shape memory takes place in single crystalline Fe–Mn–Si base alloy. It has been also found that complete shape memory can occur in polycrystalline Fe–Mn–Si base alloy through the optimization of processing conditions and chemical compositions.[13-16]

In this study we investigated the factors which determine the SME in Fe–Mn–Si based systems and designed alloy compositions which led to high corrosion resistance without decaying SME. We also show that the thermomechanical treatment improves the SME of the new alloys as in the case of Fe–Mn–Si base system.[17]

2. Experimental Procedure

The specimens were prepared by induction furnace melting in vacuum using high purity iron, manganese, silicon, chromium and nickel. Chemical compositions of alloys were in the range of 11 to 34 % Mn, 5 to 6 % Si, 0 to 13 % Cr and 0 to 8 % Ni with minor impurities: <0.01 % C, <0.005 % P, <0.01 % S in weight percent. Si content was fixed in the range of 5 to 6 % because this amount of Si was needed to obtain good SME in these alloys. Ingots were hot rolled to 16 mm in thickness after heating at 1 473 K for 1 h. The rod specimens 4 mm in diameter, 23 mm in length were cut from the plates and heated at 873 K for 10 min to eliminate the influence of machining and to memorize the shape. The magnitude of SME was evaluated by the recovered strain after tensile deformation by 2.5 to 3 % and subsequent heating to 573 K. The specimens were deformed at the rate of 1.4×10^{-4}/s using the Instron type tensile machine at room temperature. In the case of shape memory alloys which make use of stress-induced martensite, the deformation temperature affects the SME remarkably. In this study we fixed the deformation temperature to room temperature, since the alloys are deformed at room temperature for most applications. Phase transformation temperatures were determined by the change in electric resistance. Magnetic transformation temperature was determined by the change of magnetic susceptibility using a vibrating sample magnetometer.

The volume fraction of γ and ε phases was estimated by the integrated strength of corresponding characteristic peaks in X-ray diffraction.[18] Samples were sliced from the rod tensile specimens and were polished by hydrogen fluoride and hydrogen peroxide to eliminate the influence of machining and then subjected to the analysis.

The influence of thermomechanical treatment was also investigated. In this study, we employed a combination of deformation by 2 to 3 % and annealing at

873 K as the thermomechanical treatment.

Microstructures were observed with an optical microscope. The specimens were etched by nitric alcohol after polished mechanically and chemically.

3. Results and Discussion

3.1. Effects of Alloying Elements on the SME

Table 1 shows chemical compositions, phase and magnetic transformation temperature and shape memory effect of Fe–Mn–Si based systems. The effects of Cr and Ni additions are also shown. In this table recovered strains are values after initial deformation.

Figs. 1 and 2 present the effects of Mn content on the SME for Fe–Mn–Si–Cr and Fe–Mn–Si–Cr–Ni alloy systems, respectively. Fig. 3 shows that the optimum Mn content for the SME decreased as the Cr content increased. While the optimum Mn content for the SME cannot be simply determined when both Cr and Ni exist as shown in Fig. 2. We discuss this reason later.

In Fe–Mn–Si based systems, a suitable combination of Ms and T_N temperatures is critical to obtain good SME. First, the Ms temperature should lie just below the deformation temperature. When Ms temperature is high, martensite already exists in the sample and will suppress stress-induced martensitic transformation. However, when the Ms temperature is far below the deformation temperature, the stress-induced martensitic transformation is again suppressed, since too high stress is required to induce a martensite.

In Fe–Mn–Si system, the Ms temperature can be controlled by changing Mn content. However, the Néel temperature (T_N) is also strongly affected by Mn content and when T_N becomes higher than Ms, the austenite is stabilized against martensitic transformation. Mn raises T_N and reduces Ms, while Si reduces T_N without changing the Ms temperature, therefore the control of Ms and T_N becomes possible by changing the combination of Mn and Si contents. Although the control of these temperatures is possible by other alloying elements, it has been found that Si addition has two other beneficial effects;

a) to increase the strength of matrix, and

b) to reduce the stacking fault energy,

whereby Si addition is indispensable to achieve good SME.[13]

For practical applications, we need to improve other properties such as corrosion resistance. An addition of Cr is effective to improve the corrosion resistance, however, it also affects the Ms and T_N temperatures. Therefore, we need to know the effects

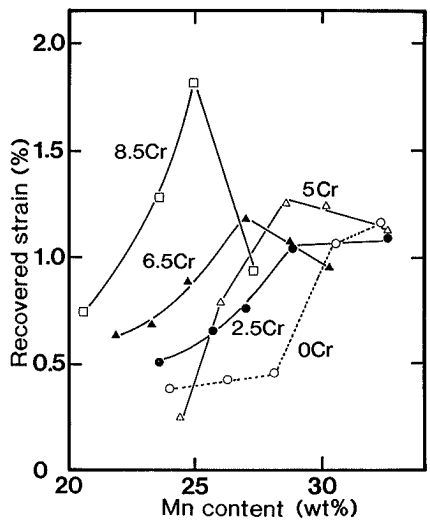

Fig. 1. Effect of Cr and Mn contents on the SME for Fe–Mn–Si–Cr system. The magnitude of SME was measured after heated to 573 K following tensile deformation by 2.5 % at room temperature.

Table 1. Composition dependence of phase and magnetic transformation temperatures and recovered strain.

Specimen	Composition (wt%)				Recovered strain (%)	Transformation temperatures (K)		
	Mn	Si	Cr	Ni		Ms	As	T_N
28Mn-6Si	28.1	5.9	—	—	0.47	343	413	264
30Mn-6Si	30.5	6.2	—	—	1.08	—	391	273
32Mn-6Si	32.3	6.0	—	—	1.17	293	388	284
26Mn-6Si-5Cr	26.0	5.9	5.0	—	0.79	299	423	230
28Mn-6Si-5Cr	28.6	6.0	5.0	—	1.26	293	392	243
30Mn-6Si-5Cr	30.2	5.9	4.9	—	1.25	—	363	255
25Mn-6Si-7Cr	24.7	5.9	6.6	—	0.89	301	392	236
27Mn-6Si-7Cr	27.0	5.9	6.8	—	1.18	—	350	243
29Mn-6Si-7Cr	28.7	6.0	6.6	—	1.06	—	342	254
18Mn-5Si-8Cr-5Ni	17.5	5.1	8.5	5.5	1.11	254	370	—
20Mn-5Si-8Cr-5Ni	20.4	5.0	8.0	5.0	2.05	261	354	178
22Mn-5Si-8Cr-5Ni	22.2	4.9	8.2	5.0	1.41	256	367	—
14Mn-6Si-9Cr-5Ni	13.6	6.0	9.2	4.8	0.97	—	400	—
15Mn-6Si-9Cr-5Ni	14.7	6.0	9.2	4.9	1.11	—	389	—
16Mn-6Si-9Cr-5Ni	15.7	5.9	9.2	4.9	1.55	—	394	—
11Mn-5Si-12Cr-7Ni	11.2	4.7	11.6	6.7	1.35	266	369	—
13Mn-5Si-12Cr-7Ni	13.0	4.7	11.4	6.8	1.64	243	367	—
16Mn-5Si-12Cr-5Ni	16.0	5.0	11.6	4.9	1.45	267	382	169

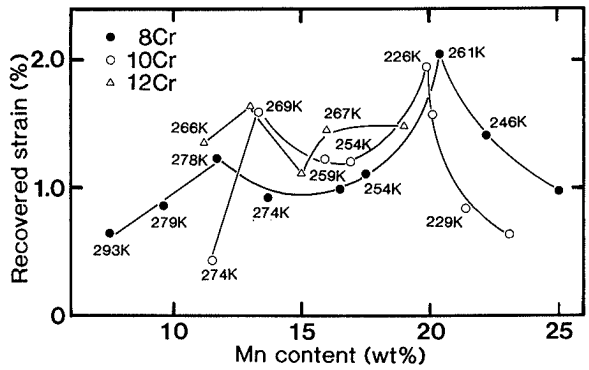

Fig. 2. Effect of Cr and Mn contents on the SME for Fe–Mn–Si–Cr–Ni system. The magnitude of SME was measured after heated to 573 K following tensile deformation by 3 % at room temperature. For reference *Ms* temperatures of the alloys are presented in the figure.

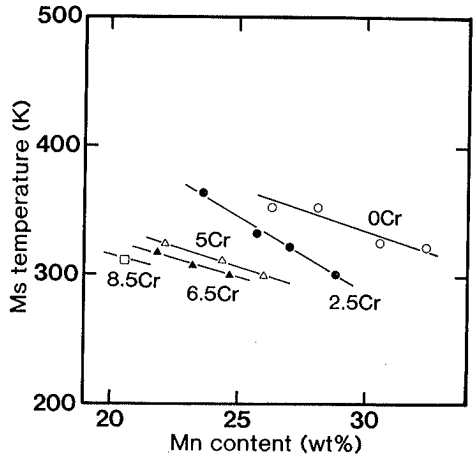

Fig. 3. Effect of Cr and Mn contents on *Ms* temperature.

of alloying elements on *Ms* and T_N for alloy design.

Fig. 3 shows the effect of Cr and Mn contents on *Ms* temperature. In order to make *Ms* temperature constant or below room temperature (the deformation temperature), we need to decrease Mn content with an increase of Cr content. While T_N temperature decreased with increase of Cr content, indicating that no care is needed for T_N in Fe–Mn–Si–Cr system.

Corrosion resistance can be enhanced with increasing Cr content. However, it was found through microscopic observation that a σ phase began to intrude into the microstructure when Cr content became more than 7 wt%. The presence of the σ phase reduced fracture toughness of the alloys and for example, although Fe–25Mn–6Si–9Cr alloy had an initial shape recovery of more than 60 % after deformed by 2.5 %, it broke when deformation and heating cycles were repeated a few times.

In stainless steels, it is well known that an addition of either Ni, C, or N is effective to suppress the formation of σ phase.[19] Since C and N produce carbide and nitride, respectively, which reduces workability, Ni seems to be the most promissing element to suppress the σ phase intrusion without decaying other properties. Therefore we investigated the SME in Fe–Mn–Si–Cr–Ni system. It is interesting to note that the optimum content could not be determined simply by considering a combination of *Ms* and T_N temperatures as already stated above. This result indicates that there exist other factors which govern the SME.

3.2. *Volume Fraction of Stress-induced Martensite and SME*

Since the SME in the Fe–Mn–Si based alloy systems is attributed to $\gamma \rightarrow \varepsilon$ martensitic transformation, the maximum volume of stress-induced ε phase must affect the SME. Actually the SME was found to depend on the amount of ε phase induced by stress.

The parent phase of Fe–Mn based alloy systems is γ (fcc structure) and the martensitic phase is ε (hcp structure). The ε phase is formed by the movement of a partial dislocation in the direction of $a/6\langle 121\rangle$ on

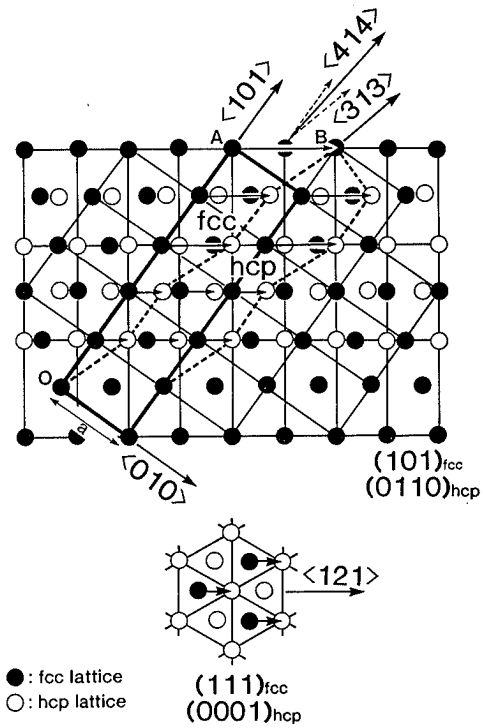

γ and ε phases are indicated with solid line and broken line, respectively.
After the transformation, about 20 % elongation is obtained ($\overline{0B}/\overline{0A}=1.23$).

Fig. 4. Schematic illustration of the transformation from γ to ε in Fe–Mn–Si based systems.

the (111) face of γ.

The movement of atoms during $\gamma \rightarrow \varepsilon$ transformation on (101) face of fcc and on (111) face of fcc is shown in Fig. 4. Assuming that the layers is stacked as *ABCABC*, the phase transformation occurs by slipping on every 2 layers by $a/6\langle 121\rangle$. When $\gamma \rightarrow \varepsilon$ transformation occurs, the region drawn with solid line transforms into the region drawn with broken line in Fig. 4. About 20 % elongation is possible in the direction of $\langle 414\rangle$ because the length of $\overline{0A}$ is elongated as that of $\overline{0B}$. The direction of $\langle 414\rangle$ can be decomposed into 2 vectors $\langle 101\rangle$ and $\langle 313\rangle$ as shown in Fig. 4. This model does not conflict with the fact that the maximum complete was obtained when deformed

in ⟨414⟩ direction in Fe–30Mn–1Si (wt%) single crystal. Considering that the crystal orientations are random in polycrystalline alloys, the average amount of recovered strain (Sr) can be estimated by the following equation.

$$Sr(\%) = 20 \times f \times (x/100) \quad \text{.....(1)}$$

Where x is the volume fraction of stress-induced martensite and the factor $f(0<f\leqq 1)$ depends on the condition of polycrystalline determined by thermal or mechanical treatment.

The recovered strain is proportional to the volume fraction of stress-induced martensite.

Fig. 5 shows the relationship between the SME and the amount of ε in Fe–xMn–6Si–5Cr(wt%) alloys. According to this figure, the alloys need to consist of only γ in the non-deformed condition and to generate a large amount of ε in the deformed state in order to have a good SME. In the alloys containing 5 wt% Cr, Ms lies near room temperature when Mn content is 28 % and the largest shape recovery is achieved.

Fig. 6 shows the relationship between the SME and the amount of ε which is introduced in Fe–Mn–Si based systems. In this figure the amount of ε indicates that formed after cooled below Ms temperature. According to this figure, recovered strain increased with increasing such amount of ε. The factor f could be evaluated as 0.28. The reason why the factor f became very low is considered to be that not only phase transformation but also slip deformation took place during deformation and hence the reverse transformation was restricted.

As mentioned above, in order to obtain good SME which originates in stress-induced martensitic transformation, alloy design must satisfy the following conditions:

(1) Ms should be lower than the deformation temperature.

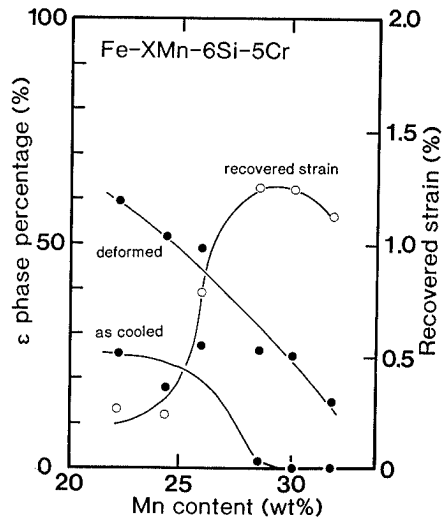

Fig. 5. Effect of the amount of ε on the SME for Fe–xMn–6Si–5Cr.
The amount of deformation is 3 %. In order to have a good SME, the alloys need to consist of only γ in the non-deformed condition and generating a large amount of ε in the deformed state.

(2) A large amount of martensite can be formed by stress-induced transformation.

The 2 peaks of the SME in Fig. 4 correspond to the point which has the maximum amount of stress-induced ε martensite and the point where Ms lies just below the deformation temperature or room temperature.

Although Ms seems to be a little too low (261 K) in Fe–20Mn–5Si–8Cr–5Ni(wt%), a fairly good shape recovery can be achieved because the amount of stress-induced ε martensite is reasonably large and being about 35 %. We believe that in this system, the difference in free energy between γ and ε is reasonably large even at room temperature despite Ms lies far below that temperature.

3.3. *Training Effect on SME*

The effect of thermomechanical treatment which consists of repetition of deformation and annealing at 873 K on the SME is shown in Fig. 7. An improvement in the SME was observed both in Fe–20Mn–5Si–8Cr–5Ni and in Fe–16Mn–5Si–12Cr–7.5Ni.

This phenomenon is known as the training effect in Fe–Mn–Si base system. It is noticeable that

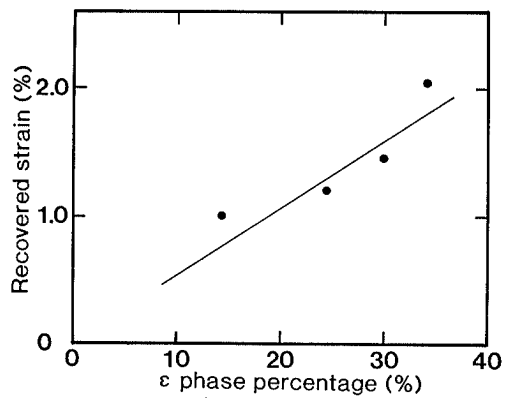

Fig. 6. The relationship between the amount of ε which can be induceed by stress and recovered strain in Fe–Mn–Si based systems.

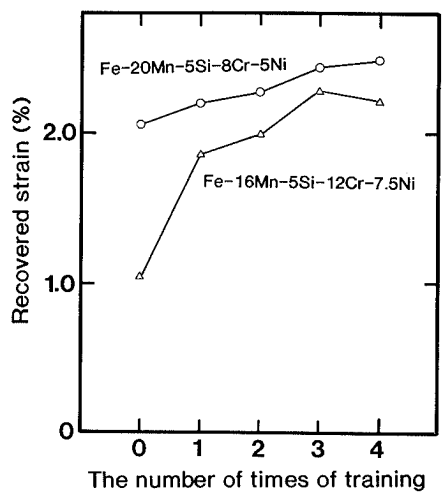

Fig. 7. Effect of the training on SME for Fe–Mn–Si–Cr–Ni system.
The training consists of the repetition of deformation by 2.5 % and annealing at 873 K.

recovered strain reaches more than twice the initial value through this treatment in Fe–16Mn–5Si–12Cr–7.5Ni alloy. Since the initial recovered strain was fairly good in Fe–20Mn–5Si–8Cr–5Ni alloy, the effect of the training was relatively small.

Fig. 8 shows the temperature dependence of yield stress for Fe–20Mn–5Si–8Cr–5Ni alloy before and after training. As in the case of Fe–Mn–Si base system, the stress for slip deformation can be increased and the stress for martensitic transformation can be decreased by the training.

Fig. 9 shows results of optical microscopic observation while training in Fe–28Mn–6Si–5Cr(wt%) alloy. After tensile deformation and annealing at 873 K, most ε martensite is formed at the same place as in the initial deformation. It is also notable that the amount of ε martensite increases after training. We believe that some structure such as stacking fault will remain in the sample and can work as a nucleation site for martensite in the following deformation and thereby reduces the stress for martensite formation. The deformation will also create some defect structures such as dislocations and leading to the increase of the resistance to slip deformation. A combination of the above 2 effects can contribute to the improvement of the shape memory effect.

4. Conclusions

In Fe–Mn–Si system, the optimum composition could be determined simply by considering a combination of Ms and T_N temperatures. However, in the Fe–Mn–Si–Cr–Ni system, we found that the volume of stress-induced martensite did not show maxi-

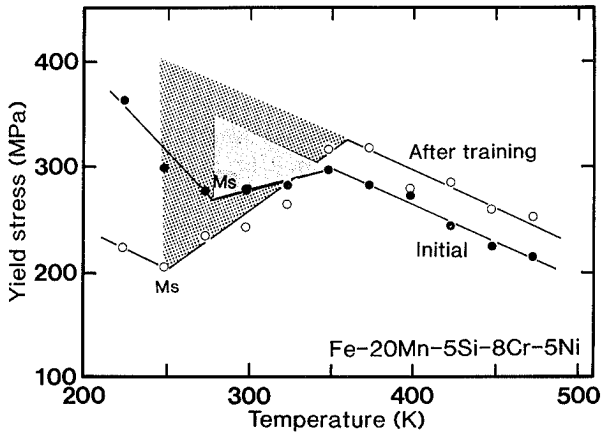

Fig. 8. Change of temperature dependence of yield stress in the training in Fe–20Mn–5Si–8Cr–5Ni alloy.

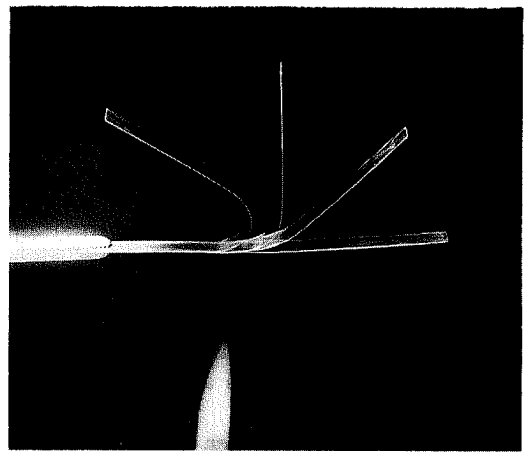

Fig. 10. Shape memory effect observed in the new alloy.

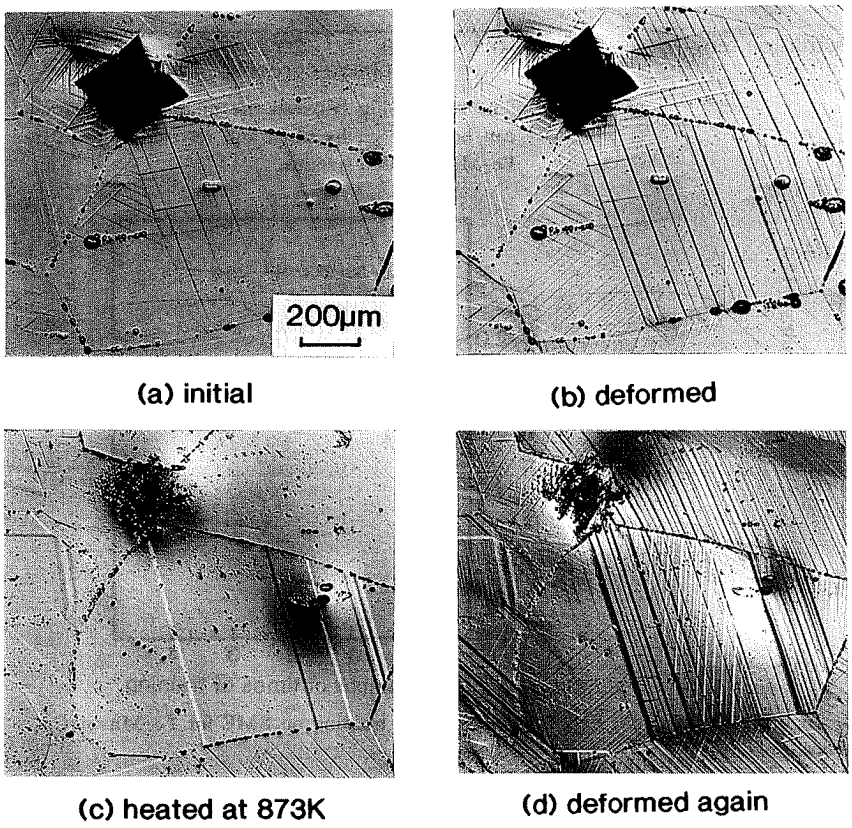

Fig. 9.
The microstructural change in the training.

mum when *Ms* lay just below the deformation temperature. We could design the new alloy system in terms of the maximum volume of stress-induced martensite. The new system exhibits good SME along with good corrosion resistance. Shape memory effect of the new alloy is shown in Fig. 10.

We have also found that the training treatments can improve the SME in the new Fe–Mn–Si–Cr–Ni system and believe that the treatment is effective to improve the SME for all the shape memory alloys which make use of the stress-induced $\gamma \rightarrow \varepsilon$ martensitic transformation.

Acknowledgments

The authors are grateful to Messrs. K. Niki and S. Yahata of Nippon Steel Corporation for their assistance in preparing samples and performing tensile tests.

REFERENCES

1) L. C. Chang and T. A. Read: *Trans. Am. Inst. Min. Metall. Pet. Eng.*, **189** (1951), 47.
2) S. Miyazaki and K. Otsuka: *ISIJ Int.*, **29** (1989), 353.
3) J. Perkins and W. E. Muesing: *Metall. Trans. A.*, **14A** (1983), 33.
4) K. Otsuka, H. Sakamoto and K. Shimizu: *Acta metall.*, **27** (1979), 585.
5) T. Sohmura, R. Oshima and F. E. Fujita: *Scr. metall.*, **14** (1980), 855.
6) C. M. Wayman: *Scr. metall.*, **5** (1971), 489.
7) S. Kajiwara: *Trans. Jpn. Inst. Met.*, **26** (1985), 595.
8) T. Maki, K. Kobayashi, M. Minato and I. Tamura: *Scr. metall.*, **18** (1984), 1105.
9) K. Enami, S. Nenno and Y. Minato: *Scr. metall.*, **5** (1971), 663.
10) A. Sato, E. Chishima, K. Soma and T. Mori: *Acta metall.*, **30** (1982), 1177.
11) A. Sato, E. Chishima, Y. Yamaji and T. Mori: *Acta metall.*, **32** (1984), 539.
12) A. Sato, Y. Yamaji and T. Mori: *Acta metall.*, **34** (1986), 287.
13) M. Murakami, H. Otsuka, H. G. Suzuki and M. Matsuda: Proc. Int. Conf. on Martensitic Transformations (ICOMAT-86, Nara), Japan Inst. Metals, Sendai, (1986), 985.
14) M. Murakami, H. Suzuki and Y. Nakamura: *Tetsu-to-Hagané*, **72** (1986), S1573; *Trans. Iron Steel Inst. Jpn.*, **27** (1987), B87.
15) M. Murakami, H. Otsuka, H. Suzuki and S. Matsuda: *Tetsu-to-Hagané*, **72** (1986), S1574; *Trans. Iron Steel Inst. Jpn.*, **27** (1987), B88.
16) M. Murakami, H. Otsuka and S. Matsuda: *Tetsu-to-Hagané*, **72** (1986), S1575; *Trans. Iron Steel Inst. Jpn.*, **27** (1987), B89.
17) H. Otsuka, M. Murakami and S. Matsuda: *MRS Int'l. Mtg. on Adv. Mats.*, **9** (1989), 451.
18) B. D. Cullity: Elements of X-ray Diffraction, Addison-Wesley, Pub. Co., Massachusetts, (1956), 388.
19) F. C. Hull: *Weld. J.*, **52** (1973), No. 5, 193.